ELSEVIER

Colloids and Surfaces A: Physicochem. Eng. Aspects 217 (2003) 33–47

COLLOIDS AND SURFACES A

www.elsevier.com/locate/colsurfa

The colloid and radionuclide retardation experiment at the Grimsel Test Site: influence of bentonite colloids on radionuclide migration in a fractured rock

A. Möri [a,*], W.R. Alexander [b], H. Geckeis [c], W. Hauser [c], T. Schäfer [c], J. Eikenberg [d], Th. Fierz [e], C. Degueldre [d], T. Missana [f]

[a] *Geotechnical Institute Ltd., Bern, Switzerland*
[b] *National Co-operative for the Disposal of Radioactive Waste (NAGRA), Wettingen, Switzerland*
[c] *Forschungszentrum Karlsruhe, Institut für Nukleare Entsorgung (FZK-INE), Karlsruhe, Germany*
[d] *Paul Scherrer Institute (PSI), Villigen, Switzerland*
[e] *Solexperts AG, Schwerzenbach, Switzerland*
[f] *CIEMAT, Madrid, Spain*

Abstract

The colloid and radionuclide retardation (CRR) experiment is dedicated to the study of the in situ migration behaviour of selected actinides and fission products in the absence and presence of bentonite colloids in a water-conducting feature (shear zone) in the Grimsel Test Site (GTS). The technical scenario considers the bentonite backfill/host rock interface as a potential source for colloids. The experiment investigates the migration behaviour of U, Th, Pu, Am, Np, Sr, Cs, I and Tc and the influence of smectitic bentonite colloids by two in situ tracer injections in a well-characterised dipole. The field experiments are supported by an extended laboratory and modelling programme. Colloid breakthrough is determined on-line by a mobile, laser-induced breakdown detection apparatus (LIBD), a mobile photon correlation spectrometer (PCS) and, afterwards in the laboratory, by a single particle counting method (SPC) using a laser light scattering technique. Bentonite colloids generated from bentonite backfill material were found to be stable in the experimental groundwater and the influence of pH and salinity on colloid stability was investigated. The in situ monitored breakthrough of the tri- and tetravalent actinides Am and Pu and of Cs followed the colloid breakthrough indicating some degree of colloid-mediated migration of these radionuclides in the experimental shear zone. But even when no colloids had been added to the tracer cocktail, part of Am(III) and Pu(IV) appears to migrate as colloids. The different colloid detection techniques revealed a colloid recovery between 80 and 90% of the injected bentonite colloids. The CRR experimental results are considered from the perspective of understanding the likely long-term behaviour of a deep geological repository for radioactive waste and as an indicator of the way forward to the next generation of in situ experiments.

Keywords: Colloid and radionuclide retardation experiment; Bentonite colloids; Radionuclides; Grimsel Test Site; In situ tracer injection

* Corresponding author. Tel.: +41-31-389-3431.
E-mail address: andreas.moeri@geo-online.com (A. Möri).

0927-7757/03/$ - see front matter
doi:10.1016/S0927-7757(02)00556-3

1. Introduction

In most high-level radioactive waste repository designs, the waste is packed in massive metal canisters which are surrounded by a large volume of bentonite clay, all of which constitute the engineered barrier system (EBS). The canisters will slowly degrade and eventually fail, releasing some radionuclides, most of which are expected to be retained and to decay within the bentonite. However, it is conceivable that, for example, gas production may induce potential flow paths in the bentonite allowing a limited amount of radionuclides to escape the EBS. Erosion of the bentonite at the EBS/host rock interface is expected to produce bentonite colloids (see Fig. 1) and any radionuclides released from the EBS may become associated with these colloids and migrate through water conducting features (e.g. shear zones) towards the biosphere.

Much information now exists on the behaviour of natural and artificial colloids in deep and shallow groundwaters but, despite this, it has not yet been possible to completely define the likely impact of colloid-facilitated transport of radionuclides released from a repository. This is partly because the potential role of colloids in radionuclide transport is quite complicated. As noted in Ref. [1], five requirements must be fulfilled (the so-called colloid ladder, see Fig. 2) to prove that colloid-facilitated transport of radionuclides in a potential repository host rock may be of significance to the long-term performance of a waste repository: colloids must be present, mobile and stable under the given groundwater conditions (geochemical and hydrogeological environment), radionuclide association with the colloids must take place and the association must be irreversible.

The colloid and radionuclide retardation (CRR) experiment is dedicated to study the in situ migration behaviour of selected actinides and fission products in the absence and presence of bentonite colloids in fractured rock at Nagra's Grimsel Test Site (GTS) in the central Swiss Alps. In addition to the programme of in situ experiments, the project partners, namely ANDRA (F), ENRESA (E), FZK-INE (D), JNC (J), USDoE/Sandia (USA) and Nagra (CH), funded an extensive programme of laboratory and modelling work. The modelling programme was focussed on calculations of radionuclide solubility in both the test site groundwater and bentonite porewater in addition to flow field modelling (geostatistical, inverse modelling of crosshole pumping tests) and reactive transport modelling (evaluation of preparatory tracer tests and predictive transport

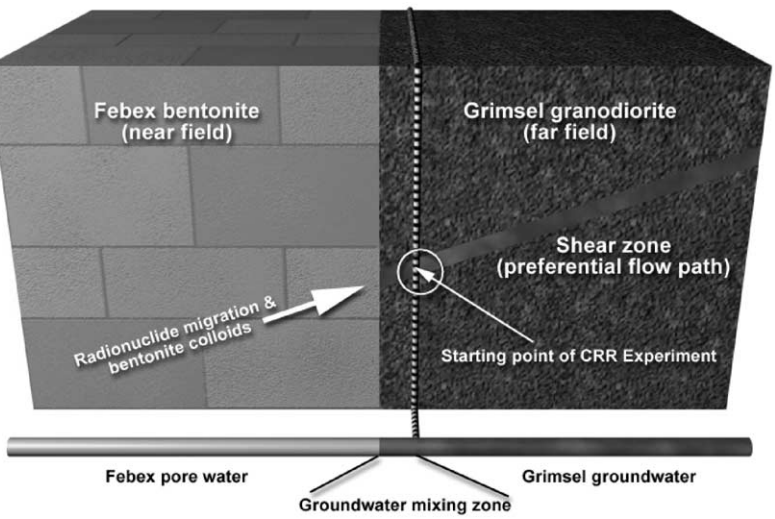

Fig. 1. Conceptual model of the CRR experiment.

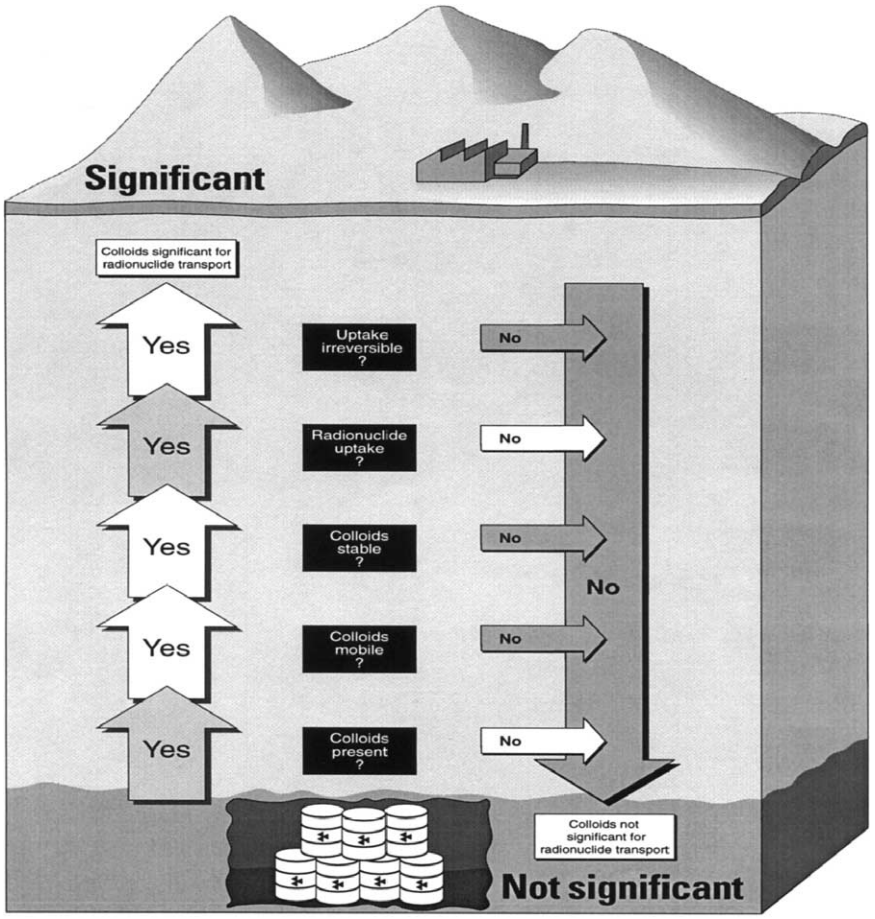

Fig. 2. The 'colloid ladder' indicates when colloid-facilitated radionuclide transport in the host rock may become significant to the long-term performance of deep geological waste repositories (from Re. [1]).

modelling). The laboratory programme concentrated on batch experiments with different solids (Grimsel granodiorite, fault infill material, bentonite, etc.) in the absence and presence of bentonite colloids. The results of the laboratory programme and predictive modelling of the in situ behaviour of the radionuclides will be compared with the in situ data on radionuclide and colloid behaviour.

Between January and March 2002, the final tracer injection campaign was carried out in a test shear zone (a complex, multi-fracture zone with fault infilling material; see Refs. [2,3] for details) at the GTS. Six tracer injections were performed with the fluorescent dye uranine in combination with the conservative radiotracer ^{131}I (the latter was intended to be used as conservative tracer, measured online, during the main injections) to compare the behaviour of both tracers and to confirm the reproducibility of the injection functions. The two main tracer injections were performed with

- $^{243}Am(III)$, $^{237}Np(V)$, $^{242}Pu(IV)$, $^{238}Pu(IV)$, $^{238}U(VI)$, $^{85}Sr(II)$, $^{131}I(I)$ and $^{232}Th(IV)$ in the absence of bentonite colloids and
- $^{241}Am(III)$, $^{237}Np(V)$, $^{244}Pu(IV)$, $^{238}Pu(IV)$, $^{233}U(VI)$, $^{99}Tc(IV)$, $^{137}Cs(I)$, $^{85}Sr(II)$, $^{131}I(I)$ and $^{232}Th(IV)$ in the presence of 20 mg l^{-1} of bentonite colloids.

Whenever possible, it was decided to use different radioisotopes of the injected elements in order to distinguish the measured element concentrations from the two runs in the outlet solutions.

The work presented here was produced by a large team of co-workers (who are identified in the acknowledgements below). The aim of this paper is to give an insight into the presently performed work related to colloid-mediated radionuclide migration studies at the GTS. Some selected experimental results of laboratory studies and in situ migration experiments are presented and discussed below in order to demonstrate the colloid relevance to the migration of some radionuclides in a given granitic environment. However, further evaluation of the data obtained in laboratory and field experiments is currently underway and several publications will follow this overview paper, describing in more detail the methodologies, results and final conclusions of the project (see Refs. [4–7]).

2. Grimsel Test Site (GTS)

2.1. Site description

The CRR in-situ experiments were carried out at Nagra's GTS which is located at about 1730 m above sea level under a ~450 m overburden of crystalline rock. The test shear zone which was selected for the CRR experiment is located at the former migration (MI) site which has the advantage of being a well characterised site due to previous work carried out there in two projects over the previous 15 years (see Refs. [8–11] for details). Fig. 3 shows the test site with the AU gallery, the boreholes and the four CRR dipoles. The preparatory tracer tests were performed in each of the four dipole flow field configurations under varying flow conditions. The dipoles consist of existing boreholes from the former Migration Experiment (MI boreholes; see Refs. [8,9] for details) and of new CRR boreholes which all have been instrumented with triple packer systems. The final tracer injections were performed in dipole 1 (see D-1 in Fig. 3) which has a straight-line length of 2.23 m.

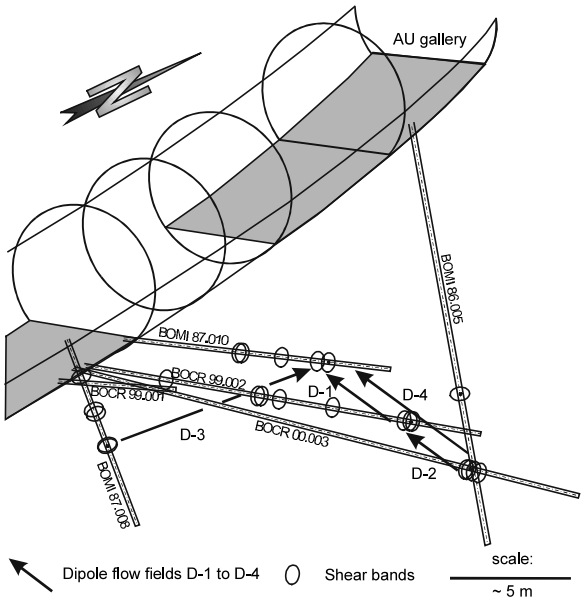

Fig. 3. 3D view of the CRR test site (viewed from the south) showing the more important boreholes used in the experiment. The plane of the page represents the idealised plane of the shear zone (the grey section in the gallery indicates the concrete floor which is missing in the area where the shear zone intersects the gallery)

2.2. Hydrogeochemical overview

The host rock of the test shear zone is the Grimsel granodiorite, which was affected by greenschist metamorphism and deformation about 25 Ma BP where the original plutonic rocks were partially metamorphosed to gneisses. The Grimsel granodiorite is medium to coarse grained and is transected by a series of shear zones and scattered lamprophyre and aplite dykes. The granodiorite consists mainly of 23 vol% quartz, 23 vol% plagioclase, 20 vol% potassium feldspar and 25 vol% sheet silicates (biotite, muscovite and chlorite). The ductile deformation, which formed extended shear zones (mylonites) was followed by brittle deformation, which can be attributed to the post metamorphic regional uplift. The CRR test shear zone is characterised as a WSW-ENE striking, steeply dipping (to the SSE) cleavage parallel shear plane. The original shear direction was sub-vertical, parallel to the mineral stretching lineation with a minimum value for shear displace-

ment of 3 m. The thickness of the shear zone varies between 0.15 and 0.90 m. Brittle reactivation of the shear zone resulted in a reduction in the internal cohesion of the shear zone and in the formation of fault infill between the sheared planes which has an increased sheet silicate content compared to the matrix and to the mylonites (about 45 vol%, for details see Ref. [2]). This increase in sheet silicates (along with the presence of secondary clay minerals produced by the greenschist facies overprint) in the fault infill and a relatively large porosity of 30–40%, are responsible for the observed (see Fig. 4 for details) preferential retardation of radionuclides in this material as seen also in the EP experiment (for details see Ref. [3]).

The evaluation of the borehole outflow tests in the MI and CRR boreholes crosscutting the test shear zone at the east side of the gallery indicated transmissivities around 10^{-6} m^2 s^{-1}. The test site groundwater is a Na^+/Ca^{2+}–HCO_3^-–SO_4^{2-} groundwater type with a pH of 9.6 and an E_h below −300 mV. The electrical conductivity is 103 μS cm^{-1} and the ionic strength 0.0012 M. The natural colloid background of the test site groundwater was found to be about 10^{10} colloids l^{-1} between 40 and 1000 nm (for details see Ref. [12]) and additional studies of the natural background are currently ongoing.

2.3. Experimental set-up

The flow field was established between the injection borehole BOCR 99.002 (10 ml min^{-1}) and the extraction borehole BOMI 87.010 (150 ml min^{-1}) and has a straight-line length of 2.23 m (see Fig. 3). The hydraulic flow along the dipole points to the gallery, thus following the natural groundwater flow towards the galleries. The packed off interval in BOCR 99.002 is 40 cm (115 ml) and in BOMI 87.010 is 31 cm (83 ml). The new CRR boreholes were arranged in a way which enables shear zone parallel overcoring of the resulting dipole flow fields from the gallery if significant amounts of tracer and/or colloids were retarded within the shear zone (cf. [3,13]).

Specially designed triple packer systems were installed in the two boreholes in such a way that the shear zone interval of the borehole was tightly sealed. The test intervals were equipped with a pressure measurement line, a flow line and a quartz fibre pair for downhole detection of the fluorescent uranine dye. In addition, all parts

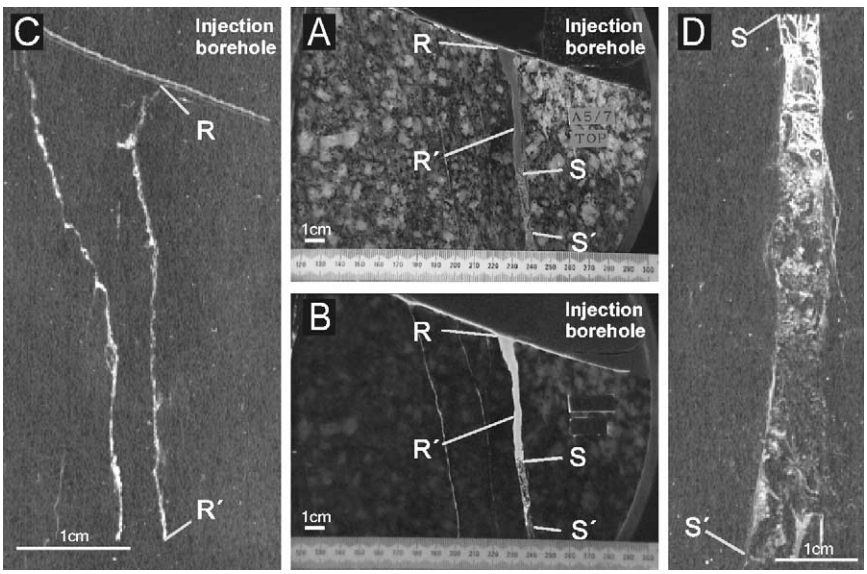

Fig. 4. (A,B) Slab photographs under normal and UV light; (C,D) α-autoradiograph images from the channel type structure. The major flow paths within the shear zone are located in the fault infill as flow channels. Note that the injected α-emitting radionuclides were preferentially retarded at the flow channel surface and within the fault infill; details in Ref. [3].

within the interval exposed to groundwater were PEEK (polyether etherketone) coated in order to minimise tracer sorption on the test equipment while using radionuclide tracers.

The injected water was in situ groundwater and was pumped with a HPLC pump through pH and E_h flow-through cells and then passed a flow meter-all instruments were directly linked to the data acquisition system. The radionuclide cocktails were injected with a newly developed tracer dosage system (see Ref. [4] for details) into the PEEK tubing of the injection line by applying a N_2 overpressure to the vial containing the cocktail. This procedure allowed avoiding the contact of the solution with the aerobic atmosphere. The actual injection flow rate (10 ml min^{-1}) was monitored by measuring the mass loss from the cocktail container.

The extraction side was also equipped with an HPLC pump, pH, O_2 and E_h flow-through cells and a flow meter (see Fig. 5). The bentonite colloids at the borehole outflow were detected on-site and on-line using a laser induced breakdown detector (LIBD) [14] and by photon correlation spectroscopy (PCS) [15]. The particle size distribution of the effluent colloids was determined off-site by using a single particle counter (SPC). On-site, real-time analysis of the ^{131}I and ^{85}Sr activity was performed by γ-spectrometry with a HPGe detector. During the two main tracer injections, about 600 samples were collected from the outflow solution for further element analysis by ICP-MS (determination of radionuclides in the extraction solution and determination of Al content as an indicator for the presence of bentonite colloids) and additional γ- and α-measurements were performed in the laboratory.

3. Preparatory laboratory testing

Different types of colloids have been considered to be relevant for the scenario defining the framework of the CRR experiment. Colloidal species can be generated in the EBS of a repository due to a variety of processes:

- corrosion of the waste container could produce metaloxide/hydroxide colloids,
- corrosion of the waste form itself might generate colloidal silica, and/or clay (from vitrified waste) or uranium or other actinide phases (from spent Pu/U or mixed fuel, MOX),
- colloidal species may be derived from the bentonite (smectite, etc.) and
- natural colloids can be present in the ambient groundwater.

Radionuclides can either attach to such colloidal species by sorption or association (heterogeneous radiocolloids) or may even be the main component of such colloids, e.g. due to polymerisation of

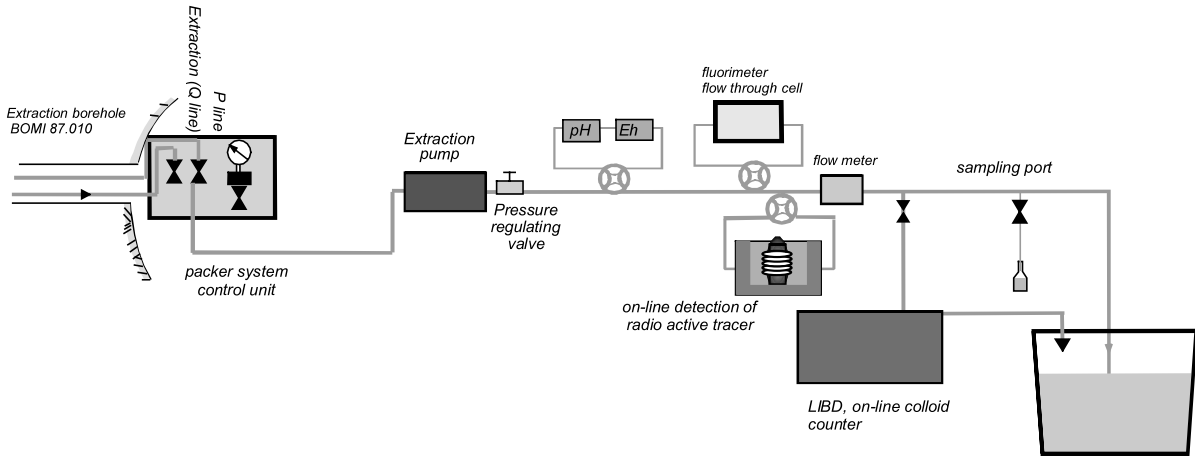

Fig. 5. Extraction borehole sampling and monitoring equipment.

hydrolysed actinide species (homogeneous radiocolloids). Laboratory studies were therefore performed with different types of colloids in test site groundwater and in the porewater of the bentonite. The experimental bentonite consists mainly of smectite (93±2%) with quartz (2±1%), plagioclase (3±1%), cristobalite (2±1%), potassic feldspar, calcite and trydimite as accessory minerals and is already in use at the GTS for the full-scale high level waste engineered barriers experiment (FEBEX, for details see Ref. [16]).

The first studies within the CRR project concentrated on the investigation of the formation of bentonite colloids at the bentonite/host rock interface, on the stability of different types of colloids and on the radionuclide uptake of the bentonite colloids.

3.1. Bentonite colloids

Bentonite colloids were obtained from crushed bentonite blocks. The material was sieved (size fraction <64 μm) and washed with Milli-Q deionised water and finally equilibrated with test site groundwater. The colloidal fraction was obtained by centrifugation. The structure of these colloids was investigated by scanning electron microscopy (SEM) techniques. SEM samples were obtained by filtering the suspension through an Amicon XM 50 membrane (pore size 3 nm), drying and subsequent covering by an Au film. The SEM image of these bentonite colloids shows that the largest number of these colloids is around 200 nm (Fig. 6, left image).

The exchange properties of bentonite colloids in the test site groundwater have been determined and the main exchangeable cations were found to be: Mg^{2+} ($\sim$31%), Ca^{2+} ($\sim$29%), Na^{+} ($\sim$29%) and K^{+} ($\sim$3%).

Two experimental set-ups have been designed in order to simulate the in situ conditions for colloid generation at the bentonite/host rock interface in the laboratory [17]: a first scenario where advection dominates colloid mobilisation (dynamic experiment) and a second where diffusion is predominant (quasi-static experiment). However, since very low flow conditions are expected to exist around the EBS in a repository, the water flow rates in the dynamic experiments were also very low (from 0.17 to 0.48 ml day^{-1}). Despite this, bentonite colloids were generated at the bentonite surface and mobilised at the bentonite/hostrock interface (for more details see Refs. [5,17]) which is in agreement also with earlier work (see, for example Ref. [18]).

The water flow at the simulated host rock/bentonite interface produced erosion on the exposed bentonite surface and solid material was found in the eluted water. The fact that the water flow actually ran at the interface, and not within the bentonite or along the external walls of the column, was confirmed by adding the fluorescent dye, uranine, to the injected water and then visually examining the sample.

The particulate matter generated at the interface contained large fragments (up to 3 μm) and smaller particles that could be clearly observed upon filtering the eluted water with a 0.45 μm pore size filter membrane. The total solid fraction was fairly polydispersed and the colloidal fraction had a mean hydrodynamic diameter, determined by PCS, ranging from 200 to 300 nm in size. Fig. 6

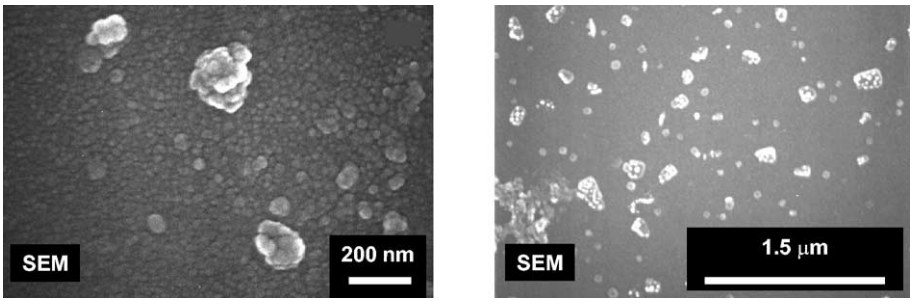

Fig. 6. Scanning electron microscope images of bentonite colloids.

(right image) shows a SEM image of a sample of the colloidal material observed in the eluted water. The 200–300 nm sized colloids (aggregates) were actually formed by smaller spherical particles. Chemical analysis, performed with EDX, identified Si, Al, Mg, Ca and Fe (probably clay minerals and metal oxides) as the main components of the colloidal material generated at the interface. The ζ potential of the colloidal material found in the eluate was always negative, and the final value lay in the expected range for smectite clay colloids of -20 and -30 mV, respectively. The concentration of both colloidal and total solid fraction generated at the interface was observed to increase with increasing water flow. It is worth mentioning that colloids were also observed in the experiments performed under quasi-static conditions which implies that colloids may be produced even in the absence of mechanical forces driving the erosion processes.

3.2. Stability of bentonite colloids

To investigate the influence of ionic strength on the stability of the Febex bentonite colloids, gradual concentration changes from 0.001 M (comparable to the ionic strength of the test site groundwater) to 0.22 M using NaCl, $NaClO_4$ or $CaCl_2$ solution were accomplished. The pH was controlled by adding NaOH or 0.1 M HCl. Fig. 7 (left image) shows the evolution of the hydrodynamic mean diameter obtained by dynamic light scattering of colloids obtained from bentonite as a function of the ionic strength of the water. An increase in the mean size clearly indicates that coagulation is occurring (in agreement with the observations in the colloid erosion experiment). The pH of the suspensions varied slightly with the addition of the electrolyte but the final values were in the range of pH 8.7 ± 0.5.

Another set of experiments was performed to study the effect of the pH and the hydrodynamic mean diameter of bentonite colloids (see Fig. 7 right image). At fixed ionic strength, the stability of the colloids strongly depends on the pH of the suspensions. The curves obtained for pH > 6 (pH 8 and 11) are flat and no substantial change in the mean size was observed during the experiment. The curve at pH 6 shows an increase of approximately 100 nm in the mean hydrodynamic diameter after 45 min whereas, at pH 5, the coagulation of colloids is practically immediate. The curve at pH 2 is very similar to the curve obtained for the fast coagulation regime at pH 5.

The pH-dependent stability behaviour of smectitic colloids depends, in fact, on the small pH-dependent charge of the amphoteric aluminol groups at the edge sites. Edge to face coagulation processes may occur at pH < 6.5 as the charge emerging at the edges is positive whereas the layer

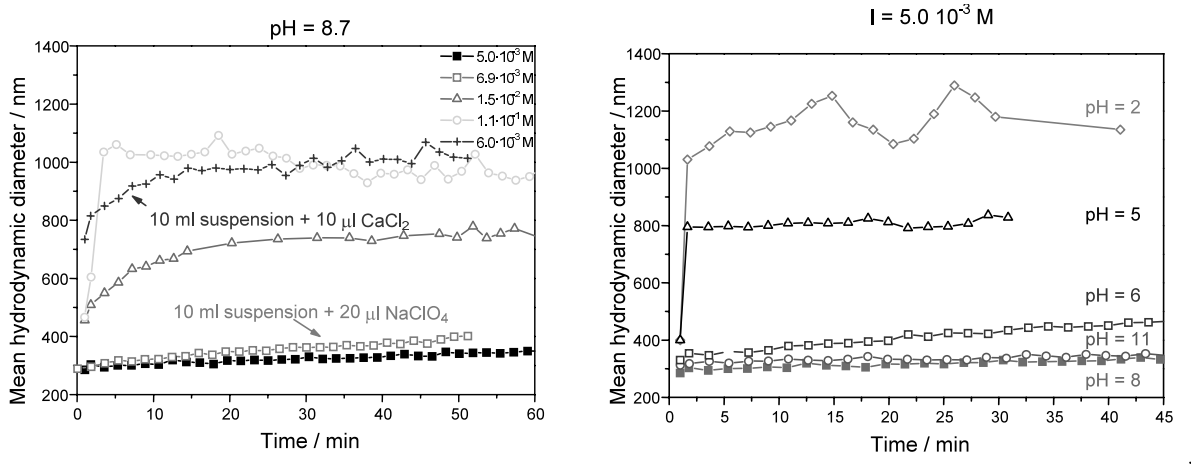

Fig. 7. Evolution of the hydrodynamic mean diameter of bentonite colloids (1.3 ± 0.3 g l^{-1}) at different ionic strengths (left) and at different pH (right).

charge at the planar face of the smectitic platelets is always negative widely independent of pH. As a consequence, bentonite colloids are expected to show high stability under the experimental groundwater conditions ($I = 10^{-3}$ M and pH 9.5) [19]. In order to verify this issue, the colloid size distribution was investigated also for longer time periods. Colloids obtained from previously washed bentonite and conditioned in the test site groundwater were prepared. The concentration of the suspension was approximately 2000 mg l^{-1}. The colloid size distribution was found to be rather invariant over a period of approximately 5 months.

3.3. Batch experiments with radionuclides and bentonite colloids

The sorption of the actinides and the fission products onto different solids, namely Grimsel granodiorite, fracture infill material and Febex bentonite colloids, was experimentally investigated in the laboratory for a number of radioelements relevant to long term safety of a repository: Cs(I), U(VI), Se(IV) and Tc(VII and IV), Am(III), Np(V) and Pu(IV and VI) (details in Ref. [5]). Not all of them were finally studied in the in situ experiment. The following main findings resulted from these studies:

- Pu, Am, U and Cs sorption on bentonite colloids is in general stronger than that found for the bulk bentonite, possibly due to the large surface area of the colloids. For the other radionuclides, sorption on the colloids appears to be much less significant. K_d-values in the range of 10^6 ml g^{-1} for Am are almost constant after short contact times similar to those for Cs ($\sim 7 \times 10^3$ ml g^{-1}), the values for Pu increase from initially 10^5 to 10^6 ml g^{-1} after 3 weeks. A similar trend is found for U where the K_d values increased from 8×10^2 to 1.5×10^3 ml g^{-1} within 12 weeks.
- Sorption of Am, Pu, Se and U on fracture infill and granodiorite displays a strong kinetic control. Even after experimental periods of 12 weeks, equilibria are not yet attained. It is not yet clear which is the dominant underlying process (redox and/or mineralisation reactions). In general, Am sorption is stronger than that of Pu and almost no sorption takes place for Np. U is much more strongly sorbed on the granodiorite than on the fracture infill. For Cs the opposite is true.
- Despite the low redox potential of the test site groundwater in the batch experiments, Np remains in oxidation state V. At least in the case of U and Se, slow reduction to oxidation state IV might contribute to the slow sorption kinetics. For Tc, a clear increase of sorption with time is found under anaerobic conditions, probably indicating that reduction to Tc(IV) occurs in the system.
- Strong sorption of Am and Pu on bentonite colloids was observed. K_d-values in the range of 10^6 ml g^{-1} for Am are almost constant after short contact times, whereas the values for Pu increase from initially 10^5 to 10^6 ml g^{-1} after 3 weeks.
- Sorption of Pu and Am onto Grimsel granodiorite or on the fault infill is decreased by more than one order of magnitude in the presence of 20 mg l^{-1} bentonite colloids. No sorption of bentonite colloids can be detected on either solid. There is some indication that actinide sorption on the bentonite colloids may be reversible, as sorption on granodiorite and fracture infill increases slightly over a time period of 1 week even in presence of the bentonite colloids.

4. In situ experiments

Eight tracer tests were performed between January and March 2002 in the test dipole. The entire test programme was performed within a very tight time plan and laboratory analyses of the field samples began immediately after in situ injections were completed.

On-site radiation protection measures were already applied during the preliminary tracer testing and were intensified during the injection of the actinides. The on-site surveillance concentrated on personal dosimetry and monitoring of potential contamination and external dose rates (note that

Table 1
Radioisotope activity, mass concentration, assumed oxidation state and colloidal fraction as determined by ultracentrifugation in radionuclide cocktails 1 and 2

	Injected activity Bq for 100 ml	Concentration (M)	Assumed oxidation state	Colloidal fraction (%)	Analytical method
Run #1 (without bentonite colloids)					
^{131}I	$7.46 \times 10^{+4}$	1.24×10^{-12}	−I	0	γ-spec.
^{85}Sr	$9.52 \times 10^{+4}$	1.28×10^{-11}	II	∼0	γ-spec.
^{232}Th	1.06×10^{-3}	1.12×10^{-8}	IV	20-30	ICP-MS
^{238}U	2.82×10^{-1}	9.50×10^{-7}	VI	0–12	ICP-MS
^{237}Np	$5.82 \times 10^{+2}$	9.44×10^{-7}	V	0–10	ICP-MS/α-spec.
^{238}Pu	$6.70 \times 10^{+2}$	4.44×10^{-11}	IV	5–58	α-spec.
^{242}Pu	$3.50 \times 10^{+1}$	9.94×10^{-9}	IV	5–58	ICP-MS
^{243}Am	$1.06 \times 10^{+3}$	5.93×10^{-9}	III	6–58	ICP-MS/α-spec.
Run #2 (incl. 20 mg l^{-1} bentonite colloids)					
^{131}I	$5.56 \times 10^{+4}$	9.23×10^{-13}	−I	0	γ-spec.
^{85}Sr	$8.24 \times 10^{+4}$	1.11×10^{-11}	II	∼0	γ-spec.
^{137}Cs	$6.07 \times 10^{+5}$	1.38×10^{-8}	I	8	γ-spec.
^{99}Tc	$6.55 \times 10^{+1}$	1.04×10^{-8}	IV	12	ICP-MS
^{232}Th	1.03×10^{-3}	1.10×10^{-8}	IV	94	ICP-MS
^{233}U	$7.22 \times 10^{+3}$	8.69×10^{-7}	VI	6	ICP-MS
^{237}Np	$6.72 \times 10^{+2}$	1.09×10^{-6}	V	0–1	ICP-MS
^{238}Pu	$7.20 \times 10^{+2}$	4.77×10^{-11}	IV	84	α-/γ-spec.
^{244}Pu	1.11×10^{-1}	6.70×10^{-9}	IV	84	ICP-MS
^{241}Am	$2.04 \times 10^{+3}$	1.15×10^{-8}	III	99	α-spec.

no contamination occurred and no doses above those expected from the natural background radiation were measured). The breakthrough solution, if not sampled, was collected within six 2000 l PVC tanks. Solid radioactive wastes were collected and transported elsewhere for handling and disposal.

4.1. Preparation of the injection cocktail

The final two radionuclide cocktails were prepared by adding the radionuclides and colloids to previously collected test site groundwater under anoxic conditions (in argon gloveboxes with <1 ppm oxygen). 125 ml of the solution were prepared and 100 ml were injected (the remaining 25 ml were used for laboratory analysis). Table 1 shows the radioisotopes used with their assumed[1] oxidation state, the injected activity and mass concentration and the colloidal fraction for each element in the injection solutions for both runs. In the injection cocktail for run 1, where no bentonite colloids had been added, colloid-bound tri- and tetravalent actinides were identified. Ultracentrifugation for 1 h at 90 000 rpm, however, yielded a considerable scatter for the colloidal radionuclide fraction, which may be due to the presence of very small colloids that cannot be sedimented under the given conditions or due to the existence of colloids of a very low density close to that of water, e.g. gel-like aggregates with a high water content. The fact that, in at least some of the ultracentrifugation experiments, colloids are detected for Pu, Th and Am indicates the relevance of colloids under these conditions.

For the second in situ experiment a 10 g l^{-1} bentonite colloid suspension was prepared by repeated suspending, centrifuging, decanting the supernatant and re-suspending the suspension in Grimsel groundwater with an ultrasound tip. The final suspension had a pH of 9.21, a specific conductivity of 117 μS cm^{-1} and a gravimetrical

[1] The oxidation states noted in Table 1 are based on thermodynamic databses and expert knowledge. In a number of cases, these were confirmed by solution speciation measurements (see Ref. [4] for details).

determined concentration of 540 ± 57 mg l^{-1}. For the injection cocktail the bentonite colloid concentration was adjusted to 20 mg l^{-1}.

The average size of bentonite colloids in the cocktail for run 2 (concentration: 20 mg l^{-1}) was 109 ± 10 nm, determined by LIBD. This time, ultracentrifugation shows clearly and reproducibly the presence of tri- and tetravalent actinides in the colloidal state, i.e. adsorbed on bentonite colloids. A small fraction of Cs also appears to be sorbed on colloids.

4.2. Breakthrough curves of the radionuclides

The determination of radionuclide concentrations in the individual samples was done by ICP-mass spectrometry (ICP-MS) and by α- and γ-spectrometry. As indicated before, only the behaviour of some of the injected radionuclides will be discussed here (for details see Refs. [4–7]).

Two main groups of breakthrough curves could be distinguished in run 1 where no bentonite colloids were added (Fig. 8): the peak maxima for tri- and tetravalent Am and Pu respectively appear about 10 min earlier than those found for the conservative non sorbing tracer ^{131}I. Twenty to thirty percent of the injected Am and Pu were recovered, which is clearly less than found for ^{131}I ($> 90\%$). It was already observed in preparatory in situ tracer tests that, in the test shear zone, colloids migrated slightly faster than the conservative tracers [14]. Therefore, it could be concluded that a certain fraction of the reduced actinides might form homogeneous or heterogeneous radiocolloids, even in the absence of added bentonite colloids and it is reasonable to speculate that the recovered Am and Pu simply represents the colloidal fraction of the injection cocktail.

Fig. 9 shows resulting breakthrough curves obtained by the measurements performed after run 2.

Again, there is a significant difference between the peak times of the tri- and tetravalent elements and the conservative tracer ^{131}I. The peak time of the more rapidly eluted radionuclides coincides with the peak time of the bentonite colloids, detected by LIBD, PCS and SPC (see below) and are not very different from those in run 1. This confirms the run 1 interpretation that a considerable fraction of the tri- and tetravalent elements was transported in a colloidal state. The main difference in the findings obtained from run 2 as

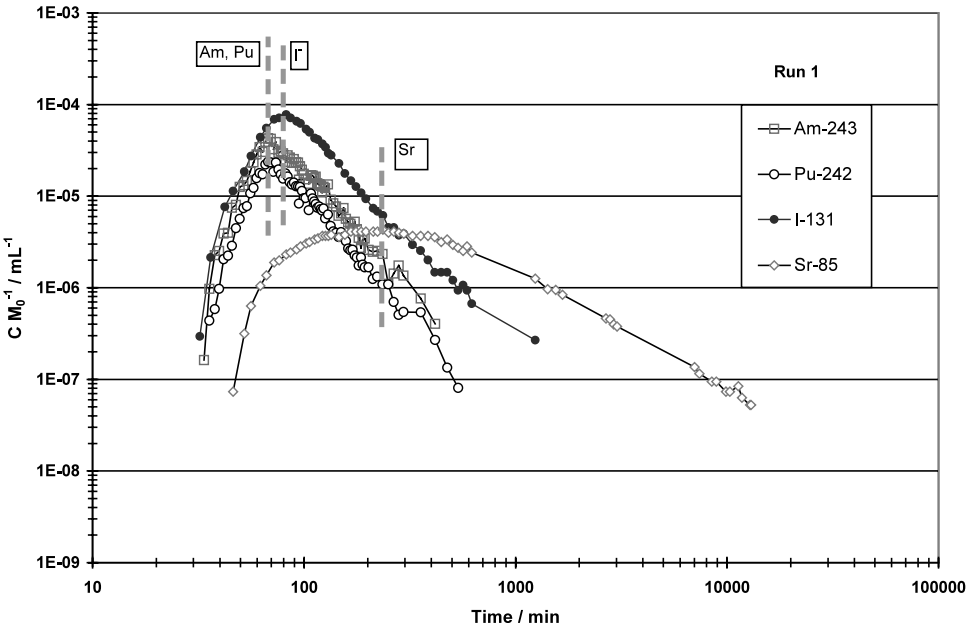

Fig. 8. Breakthrough curves of ^{243}Am, ^{242}Pu, ^{131}I and ^{85}Sr (run 1) without bentonite colloids.

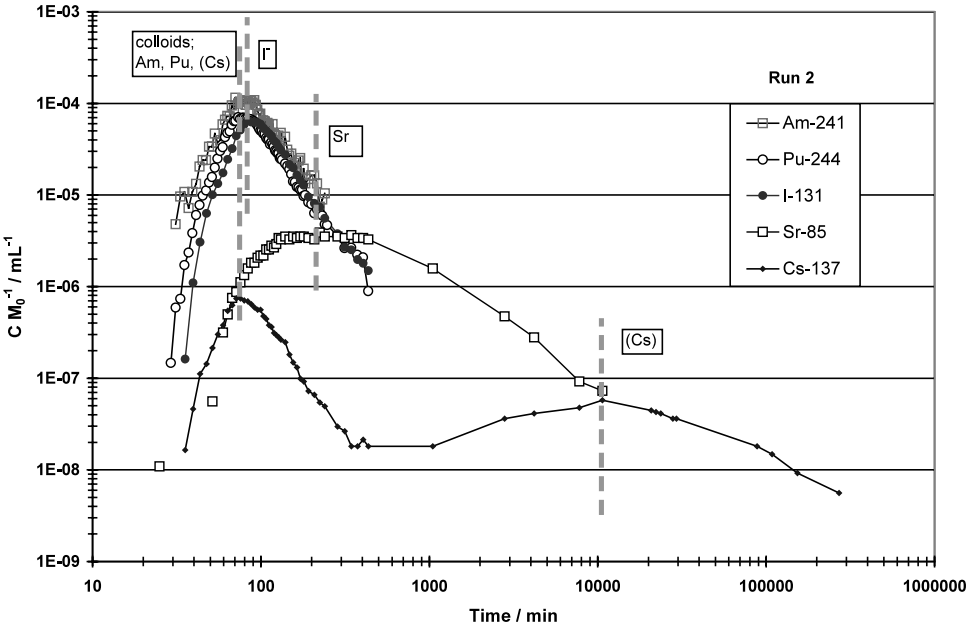

Fig. 9. Breakthrough curves of ^{241}Am, ^{244}Pu ^{131}I, ^{85}Sr and ^{137}Cs (run 2) with bentonite colloids.

compared to run 1 is the increased recovery of the tri- and tetravalent actinides (see Table 2). This is easily explained by the predominantly colloidal state of these metal ions as revealed by the ultracentrifugation experiment. This explanation is supported by the almost identical breakthrough curves obtained for ^{244}Pu and the colloids shown in Fig. 10. Cs clearly shows two different peaks (see Fig. 9) indicating that a certain fraction of this element was probably transported in a colloid state (first peak) while a second fraction appeared retarded. This interpretation is supported by laboratory ultracentrifugation tests (see Ref. [5] for details). Sr experiences a retardation during migration through the fracture due to sorption to fracture surfaces as already observed in earlier migration experiments (e.g. [8]).

4.3. Colloid analysis in breakthrough solutions

Breakthrough curves for the bentonite colloids and the curve for ^{244}Pu fit quite well and the peak maximum is slightly shifted to earlier elution times compared to the peak of the conservative tracer ^{131}I (Fig. 10), as expected from analogy to earlier colloid in situ experiments [14]. Slightly different colloid recoveries obtained by the different methods are partly due to the analytical uncertainties of the methods (notably, the PCS measurements are close to the detection limit of the method) and partly due to uncertainties given by the difficulty of precisely defining the colloid background baseline. However, consideration of the SPC, PCS, ICP-MS and LIBD data suggests that 80–90% of the colloids are passing through the test shear zone with little significant retardation. The precise mechanisms involved are currently unclear and are being further investigated in the laboratory (results will be reported in Ref. [6]).

Single particle counting revealed that the natural colloid background in the Grimsel migration groundwater was 2.1×10^5 ml^{-1} for sizes of 50–100 nm and 6.25×10^6 ml^{-1} for the same size range during the breakthrough of the bentonite colloids. The recovery of the smallest measured colloids by this technique revealed a nearly complete recovery for this size class of between 90 and 100%.

Table 2
Calculated recoveries of Am, Pu, Sr and I in run 1 and 2

Element	Run 1 (without bentonite colloids) Element recovery (%)	Run 2 (with bentonite colloids) Element recovery (%)
Am(III)	34±4	70±15
Pu(IV)	21±3	86±9
Sr(II)	87	90
I(I)	100	92

Under the experimental conditions employed here, there is short-term retardation of certain tracers within the experimental shear zone. Calculations (see Ref. [4]) show that the retarded portion of the tracers are slowly eluted over a period of several weeks at very low concentrations (several orders of magnitude below the detection limits of the analytical techniques).

5. Summary and conclusions

The presented experimental findings show that, under the given conditions in the test shear zone, bentonite colloids influence the in situ retardation behaviour of tri- and tetravalent actinides in a significant way. In the laboratory, it was confirmed that, depending on the advective flow rate of the host rock groundwater, bentonite colloid formation at the bentonite/host rock interface can occur and, thus, substantiate the colloidal scenario taken as a basis of the experimental layout. Once such colloids are produced, their stability, which is strongly dependent on the pH and salinity of the groundwater, is very high in the test site groundwater. The in situ experiment confirmed the laboratory results and the injected bentonite colloids showed a recovery of 80–90% after passing through the 2.23 m long dipole flow field. Colloid facilitated transport was shown to be faster than the transport of dissolved species. The migration behaviour of the tri- and tetravalent actinides Am and Pu was strongly mediated by the bentonite colloids and recovery increased from 20 to 30% in the absence of bentonite colloids, to about 60–80% in the presence of bentonite colloids. A part of Cs follows that behaviour while the Sr breakthrough can be explained by reversible sorption to fracture surfaces without significant interaction with colloids. Data for the migration of Np(V) and U(VI) are currently evaluated and

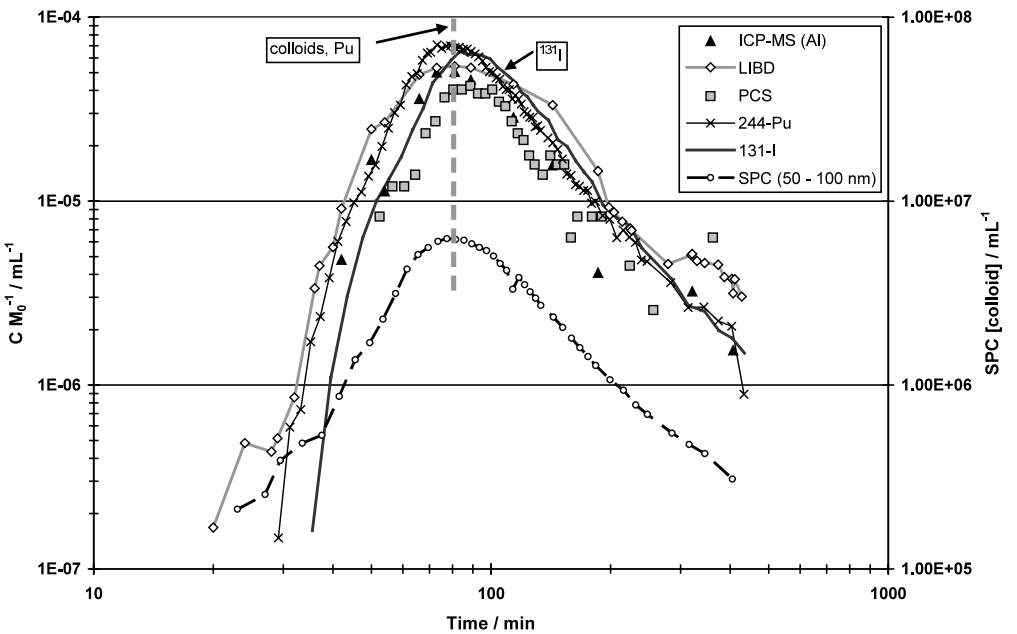

Fig. 10. Colloid breakthrough curves detected by LIBD, PCS, SPC and ICP-MS compared with the breakthrough of ^{131}I and ^{244}Pu (SPC data in colloids ml^{-1}); in case of ICP-MS detection, Al is measured as representing the bentonite colloids.

require some more interpretation. These results will be reported in a forthcoming paper.

As noted above (see Fig. 2), five requirements must be fulfilled to prove that colloid-facilitated transport of radionuclides in a potential repository host rock may be of significance to the long-term performance of a waste repository. The results presented here for the CRR test shear zone conditions indicate that the answer to the first four questions above is probably affirmative. However, before any conclusive statements can be made about the likelihood of significant colloid-facilitated radionuclide transport in the vicinity of a deep geological waste repository, two further points must be addressed:

- first, the last question about reversibility or irreversibility of radionuclide-colloid association must be investigated further in a simple system such as the CRR test shear zone and
- second, this, and the other processes examined here in CRR, must be investigated in repository-relevant systems.

Although the in situ work carried out to date has been on a longer temporal and spatial scale than laboratory experiments, the flow system transmissivities tested in URLs are usually much higher than would be expected in a suitable repository host rock (e.g. in the CRR test shear zone, the transmissivity is around 10^6 times greater). This is common with in situ work carried out and ongoing around the world today and is simply a question of practicalities (i.e. conducting in situ experiments within reasonable time scales and budgets; see examples of this in Ref. [11]). Nevertheless, even if process and mechanism understanding for colloid migration and colloid facilitated radionuclide transport has now increased (through complex experiments such as CRR), future work must consider significantly longer time scales than has been the case so far and focus on, for example, semi-stagnant groundwater systems, to try to better match the conditions in and around a waste repository. Although at an early stage, proposals are currently under consideration for the next period of work at the GTS (phase VI) for experimental durations of up to several decades — or several orders of magnitude longer than has been the case in any rock laboratory anywhere in the world to date. Further information and regular updates will be available on www.grimsel.com.

Acknowledgements

The authors would like to thank the following people for their significant contribution to the work described in this paper F. Geyer, R. Goetz, Th. Rabung and Ch. Marquardt (FZK); M. Rüthi, G. Kosakowski and A. Laube (PSI); V. Fernández, M.G. Gutiérrez, U. Alonso and M. Mingarro (CIEMAT) and F. van Dorp (NAGRA). Special thanks go also to the funding organisations, namely Nagra (CH), ANDRA (F), ENRESA (E), BMWi/FZK-INE (D), JNC (J) and USDoE/SANDIA (USA).

References

[1] W.M. Miller, W.R. Alexander, N.A. Chapman, I.G. McKinley, J.A.T. Smellie, Geological Disposal of Radioactive Wastes and Natural Analogues. Waste Management Series, vol. 2, Pergamon, Amsterdam, 2000.
[2] P. Bossart, M. Mazurek, Grimsel Test Site: Structural Geology and Water Flow-Paths in the Migration Shear Zone. Nagra Technical Report 91-12, Nagra, Wettingen, Switzerland, 1991.
[3] A. Möri, B. Frieg, K. Ota, W.R. Alexander (Eds.), The Nagra-JNC In Situ Study of Safety Relevant Radionuclide Retardation in Fractured Crystalline Rock III: the RRP Project Final Report, Nagra Technical Report NTB 00-07, Nagra, Wettingen, Switzerland, 2002, in preparation.
[4] A. Möri (Ed.), The CRR Final Project Report Series: 1—Description of the Field Phase-Methodologies and Raw Data Nagra Technical Report NTB 03-01, Nagra, Wettingen, Switzerland, 2003, in preparation.
[5] H. Geckeis, T. Missana (Eds.), The CRR Final Project Report Series: 2—Results of the Supporting Laboratory Programme Nagra Technical Report NTB 03-02, Nagra, Wettingen, Switzerland, 2003, in preparation.
[6] J. Guimerà, G. Kosakowski (Eds.), The CRR Final Project Report Series: 3—Results of the Supporting Modelling Programme Nagra Technical Report NTB 03-03, Nagra, Wettingen, Switzerland, 2003, in preparation.
[7] W.R. Alexander, A. Möri (Eds.), The CRR Final Project Report Series: 4—Project Overview and Synthesis of

Results Nagra Technical Report NTB 03-04, Nagra, Wettingen, Switzerland, 2003, in preparation.

[8] U. Frick, W.R. Alexander, B. Baeyens, P. Bossart, M.H. Bradbury, CH. Bühler, J. Eikenberg, Th. Fierz, W. Heer, E. Hoehn, I.G. McKinley, P.A. Smith, The Radionuclide Migration Experiment—Overview of Investigations 1985–1990, Nagra Technical Report NTB 91-04, Nagra, Wettingen, Switzerland, 1992.

[9] P.A. Smith, W.R. Alexander, W. Heer, P.M. Meier, B. Baeyens, M.H. Bradbury, M. Mazurek, I.G. McKinley, The Nagra-JNC In Situ Study of Safety Relevant Radionuclide Retardation in Fractured Crystalline Rock I: The Radionuclide Migration Experiment—Overview of Investigations 1990–1996, Nagra Technical Report NTB 00-09, Nagra, Wettingen, Switzerland, 2001.

[10] P.A. Smith, W.R. Alexander, W. Kickmaier, K. Ota, B. Frieg, I.G. McKinley, Development and Testing of Radionuclide Transport Models for Fractured Rock: Examples from the Nagra/JNC Radionuclide Migration Programme in the Grimsel Test Site, Switzerland, J. Contam. Hydrol. 47 (2001) 335–348. Also published in Japanese in JNC Technical Review 11, JNC TN1340 2001-006, JNC, Tokai, Japan.

[11] W.R. Alexander, P.A. Smith, I.G. McKinley, Modelling radionuclide transport in the geological environment: a case study from the field of radioactive waste disposal, in: E.M. Scott (Ed.), Modelling Radioactivity in the Environment, Ch. 5, Elsevier, Amsterdam, 2002, in press.

[12] C. Degueldre, B. Baeyens, W. Goerlich, J. Riga, J. Verbist, P. Stadelmann, Colloids in water from a subsurface in granitic rock, Grimsel Test Site, Switzerland Geochim. Cosmochim. Acta 53 (1989) 603–610.

[13] W.R. Alexander, B. Frieg, K. Ota, P. Bossart, The RRP project: investigating radionuclide retardation in the host rock, Nagra Bull. 27 (1996) 43–55.

[14] W. Hauser, H. Geckeis, J.I. Kim, Th. Fierz, A mobile laser-induced breakdown detection system and its application for the in situ-monitoring of colloid migration, Colloids Surf. A: Physicochem. Eng. Aspects 203 (2002) 37–45.

[15] M. Plaschke, T. Schäfer, T. Bundschuh, T. Ngo Manh, R. Knopp, H. Geckeis, J.I. Kim, Size characterization of bentonite colloids by different methods, Anal. Chem. 73 (2001) 4338–4347.

[16] F. Huertas, J.L. Fuentes-Cantillana, F. Jullien, P. Rivas, J. Linares, P. Fariña, M. Ghoreychi, N. Jockwer, W. Kickmaier, M.A. Martinez, J. Sampe, E. Alonso, F.J. Elorza, Full Scale Engineered Barriers Experiment for a Deep Geological Repository for High-Level Radioactive Waste in Crystalline Host Rock, EC Final report EUR 19147, EC, Luxembourg, 2000.

[17] T. Missana, U. Alonso, M.J. Turrero, Generation and stability of bentonite colloids at the bentonite/granite interface of a deep geological radioactive waste repository, J. Contam. Hydrol. (2002) in press.

[18] Japan Nuclear Cycle Development Institute, Properties of the buffer, in: H12: Project to Establish the Scientific and Technical Basis for HLW Disposal in Japan, Supporting Report 2: Repository Design and Engineering Technology, Appendix B, JNC Technical Report, JNC TN1410 2000-003, JNC, Tokai, Japan, 2000.

[19] T. Missana, A. Adell, On the applicability of DLVO theory to the prediction of clay colloids stability, J. Colloid Interface Sci. 230 (2000) 150–156.